Journal of Systems Engineering and Electronics
Vol. 29, No. 5, October 2018, pp.995 – 1008

Towards optimal recovery scheduling for dynamic resilience of networked infrastructure

WANG Yang[1], FU Shanshan[2], WU Bing[1], HUANG Jinhui[1], and WEI Xiaoyang[3,*]

1. Intelligent Transportation System Research Center, Wuhan University of Technology, Wuhan 430063, China;
2. College of Ocean Science and Engineering, Shanghai Maritime University, Shanghai, 201306, China;
3. Department of Civil and Environmental Engineering, National University of Singapore, Singapore 118414, Singapore

Abstract: Prior research on the resilience of critical infrastructure usually utilizes the network model to characterize the structure of the components so that a quantitative representation of resilience can be obtained. Particularly, network component importance is addressed to express its significance in shaping the resilience performance of the whole system. Due to the intrinsic complexity of the problem, some idealized assumptions are exerted on the resilience-optimization problem to find partial solutions. This paper seeks to exploit the dynamic aspect of system resilience, i.e., the scheduling problem of link recovery in the post-disruption phase. The aim is to analyze the recovery strategy of the system with more practical assumptions, especially inhomogeneous time cost among links. In view of this, the presented work translates the resilience-maximization recovery plan into the dynamic decision-making of runtime recovery option. A heuristic scheme is devised to treat the core problem of link selection in an ongoing style. Through Monte Carlo simulation, the link recovery order rendered by the proposed scheme demonstrates excellent resilience performance as well as accommodation with uncertainty caused by epistemic knowledge.

Keywords: dynamic resilience, network model, component importance, recovery scheduling, epistemic uncertainty.

DOI: 10.21629/JSEE.2018.05.11

1. Introduction

Networks have been a ubiquitous model to characterize the structures, functions and dynamics of modern critical infrastructures [1]. Besides the explicit network formation of many public infrastructures such as power grid, transportation and telecommunication, the major advantage of the network model lies in the ability to depict the interlaced relations among multiple components of the system, as well as the scaling and evolution of the ensemble. Analysis of network models originally has its roots in the classic graph theory. In the past twenty years, the study tends to lay stress on the large-scale statistical and dynamical properties of the network structure and the elements, which coincides with the growing complexity of the real-world systems [2].

Since critical infrastructures always play crucial roles in the fundamental aspects of the society, the safety/reliability of critical infrastructures are greatly concerned by researchers and practitioners [3]. In the literature, there have been several highly related mindsets regarding the safety of critical infrastructures, such as robustness, survivability, and flexibility. The subtle differences of these conceptual description about safety issues are addressed extensively in various research domains [4]. Recently, the study on system resilience has gained keen attention in many industrial fields [5]. This new focus of research interests is driven by the advantages offered by the resilience perspective, i.e., embracing the holistic thread to deal with the all-phase behavior of the system in the context of the disruptive event. In view of this, system resilience can be recognized in principle as the capability to plan and prepare for, absorb, respond to, and recover from disasters, in spite of the diverse definitions maintained by different researchers [6].

Earlier research on resilience mainly focuses on the qualitative side of the issue [7]. System performance prior to, during, and following a disturbance involves state transitions from normal to degrading and finally to leaping back, which is intuitively appealing but lacks the quantitative basis for further systematic planning/assessment. To ameliorate this shortcoming, three constructive methodologies are put forward: i) Use time-dependent critical functionality (also called system level delivery function or figure-of-merit [8,9]) to measure the system well-being; ii) Use expert elicitation of subjective knowledge to describe the dynamic behavior of the system compo-

Manuscript received August 01, 2017.
*Corresponding author.
This work was supported by the National Natural Science Foundation of China (51479158) and the Fundamental Research Funds for the Central Universities (WUT: 2018III061GX).

nents in terms of uncertainty representation, usually in stochastic form [10]; iii) Determine the structural dependence or constraints that govern the collective performance of individual components and the overall system [11]. These methodologies are synthesized to enrich the theoretic framework of resilience-based design and evaluation for large systems.

Network-based resilience analysis makes a favored quantitative approach upon which the aforementioned methodologies can be applied in an integrated manner [12]. There has been much research work carried out in this line of research. Gao et al. employed the dynamical system equations to describe the high-dimensional parameter space [11]. The network matrix was incorporated into the dynamic equations as an additional term to account for the interactions among the involved entities. Ganin et al. used the critical functionality as the primary factor to compute the resilience of the network, and test two types of networks with various parameters and disruptive scenarios [8]. The existing research work shows that calculation of resilience can hardly obtain a closed-form expression due to the complexity, and simulation-based analysis is the tangible way to render useful results.

In the network resilience domain, the components of the system are modeled as nodes or links, and the disruptive event is represented as a failure or degrading of some nodes and links, which causes reduced functionality at the network level [13,14]. It is easy to perceive that the importance or criticality varies with different individual components due to their internal or external features such as fragility, capacity and topological properties. This entails the revisit to the component importance (CI), which has been a well-studied term in the reliability research [15,16]. Rose divided resilience to static resilience and dynamic resilience [17,18]. The former stands for system's capability to maintain its function against disruptive events, while the latter refers to the speed at which the system recovers from disruption. In this regard, in the context of resilience study, the component importance measure (CIM) problem can be viewed with opposite angles: If the component is struck by a disruptive event, how much loss will it bring to the system? And if the disrupted component is recovered, how much benefit will it bring to the system?

These two questions are apparently inversely related, yet the assessment and treatment may show substantial differences. For the first question, it is usually investigated under the presumption that other components are intact, and the research aims at balancing the protection and prevention of the components with different importance in order to retain a lower negative impact on the whole system. For the second question, the study is geared to prioritize the recovery process of the components affected by disruptions that the overall restoration can be effective as possible. Hence, it is understandable that, due to the differences in criterion and measure, the calculation of CI can bring out incongruent results in terms of CI rankings.

Recently, research on the above problems has emerged extensively with the proliferative study on system resilience. Barker et al. investigated the CIM with respect to the overall system service recovery time [19]. Two stochastic terms were specially considered, namely the link reduction under disruption and the recovery time of the damaged link. The research constituted a stepping stone for their follow-up work [20], in which the optimization of recovery was formalized by probability inequality. Fang et al. proposed a deterministic approach to elaborate the problem in their latest research [21]. This work also used system performance curve to evaluate the overall resilience, and the real time system performance was also considered, meaning that the successive recovery of links was reflected in the performance function. One of the remarkable contributions of the work is that the optimal recovery strategy can be transformed into a family of mix integer programming under some simplifications.

The present paper aims to study on the post-hazard reaction to maximize the resilience of the network. To this end, the recovery strategy is treated as a multi-stage decision-making process in which the resources are devoted to the disrupted components such that the recovery can bring out the best effectiveness by measure of resilience. The proposed work is inspired by the concerns over the prior work, and can be ascribed to three waypoints:

(i) The uncertainty factors need to be fully considered [22]. It is presumably granted that the analyst has epistemic knowledge/estimation about the magnitude of the disruptive events and the recovery cost of individual components [23].

(ii) The recovery process is realized in an ongoing style [24]. In another word, the actual recovery status can have impact on the next decision-making, hence this idea does not follow a fixed to-do list.

(iii) From the practical point of view, the scheme should be computationally feasible.

The remainder of this article is organized as follows. Section 2 introduces the network model of generic critical infrastructure and the definition of critical functionality therein, which constitutes the formulization basis for the problem of interest. In the subsequent section, the core algorithms of this paper are sketched from simple to more general cases, and the rationality of devising the algorithms is also delineated. Afterwards, the performance of the proposed scheme is examined by a series of Monte Carlo tests, the difference and relation between the current work and the prior CI based study are discussed. In the final sections, some conclusions and suggestions for future work are presented.

2. Preliminary terminology and concept

Let $G = (N, L)$ be the network (basically a graph) comprising a set of nodes $N = \{N_i | 1 \leqslant i \leqslant n\}$ connected by a set of links $L = \{L_i | 1 \leqslant i \leqslant m\}$, where $n, m \in \mathbf{N}$. To make the problem tractable, the analysis in the sequel focuses on directed acyclic graph (DAG). For the general cases such as the multigraph or cyclic, it is envisioned that the results can be reused in these cases through decomposition of the graph. Under the DAG presumption, the link set L can be equivalently written as $L = \{l_{ij}\}$, in which $1 \leqslant i, j \leqslant n$, and each $l_{ij} \in L$ means there is a directed link from N_i to N_j. Let $\mathrm{Path}(N_i, N_j)$ be the path set of nodes N_i and N_j, in which a path is a sequence of ordered directed links starting from N_i to N_j such that no node along the links is visited more than once. $\mathrm{Path}(N_i, N_j)$ can be an empty set when no path can be found connecting N_i to N_j. Denoted by $w_{ij} \in \mathbf{R}$ the capacity of link l_{ij}, which remains a constant in the rest of discussion. Moreover, discrete time slots are considered for the time variable t, in which $t = 0$ is the initial time when system is in normal operation condition. As for the properties of a specific link, let $RA_t(l_{ij})$ be the current residual availability of link l_{ij} at time slot t. For any link and at any time, $0 \leqslant RA_t(l_{ij}) \leqslant w_{ij}$.

From the perspective of resilience, the critical functionality and the resilience metric are the fundamental quantity for further calculation [25]. With the network resilience model, the present work employs the connectivity breadth between key nodes as the critical functionality. This metric is in consistence with the real-world critical infrastructures such as the road traffic and power transmission. For the resilience metric, the definition in Fang's work [21] is inherited to feature the process of critical functionality by the integral over time horizon.

Let $\Theta = \{\langle N_p, N_q \rangle\}$ be the set of O-D pairs of interest such that $N_p, N_q \in N$, and $\mathrm{Path}(N_p, N_q) \neq \varnothing$ [26]. Notice that Θ does not necessarily exhaust all the node pairs that are connected by at least one path. Let $Wd_t(N_p, N_q)$ be the breadth of the link availability along the path of N_p and N_q at time t, standing for the aforementioned real time connectivity breadth between the two nodes. Formally, let node sequence $\{N_{p_i}\}_{i=1,2,\ldots,K}$ be one path from N_{p_1} to N_{p_K}, denoted by $\mathrm{Bot}_t(\{N_{p_i}\}_{i=1,2,\ldots,K}) = \min\limits_{i=1,\ldots,K-1}[RA_t(l_{p_i p_{i+1}})]$ the bottleneck residual availability along the path $\{N_{p_i}\}$ at time t. For the given node N_p and N_q, $Wd_t(N_p, N_q) = \sum\limits_{SP \in \mathrm{Path}(N_p, N_q)} [\mathrm{Bot}_t(SP)]$.

In interpretative words, connectivity breadth between the two nodes is the bottleneck of the widest path that connects the two nodes. This definition of connectivity breadth is analogous to the 1-norm in vector space. Alternatively, one can use other types of norm, such as $Wd_t^{\infty}(N_p, N_q) = \max\limits_{SP \in \mathrm{Path}(N_p, N_q)} [\mathrm{Bot}_t(SP)]$. In what follows, the work focuses on the first norm, but the main ideas of the research is expected to be applicable to other norms.

Let $\overline{Wd}(N_p, N_q)$ be the breadth in normal state when no link is suffering from any damage. It bears mentioning that calculation of the bottleneck between two nodes is analogous to the shortest path problem with the same complexity as the classic Dijkstra algorithm, namely $O(|N|^2)$.

The critical functionality is defined as

$$F_\Theta(t) = \sum_{\langle N_p, N_q \rangle \in \Theta} Wd_t(N_p, N_q) \tag{1}$$

and let $\overline{F}_\Theta = \sum\limits_{\langle N_p, N_q \rangle \in \Theta} \overline{Wd}(N_p, N_q)$ be the normal connectivity breadth sum for Θ. The complexity of computing $F_\Theta(t)$ is thus $O(|N|^2|\Theta|)$. With these notations, the system resilience against the disruptive event is defined by

$$R(E) = \frac{\int_0^{T_c} [F_\Theta(\tau) - F_\Theta(t_d)]\mathrm{d}\tau}{\int_0^{T_c} [\overline{F}_\Theta - F_\Theta(t_d)]\mathrm{d}\tau} = \frac{\int_0^{T_c} [F_\Theta(\tau) - F_\Theta(t_d)]\mathrm{d}\tau}{T_c \cdot [\overline{F}_\Theta - F_\Theta(t_d)]} = \frac{\int_0^{t_d} [F_\Theta(\tau) - F_\Theta(t_d)]\mathrm{d}\tau + \int_{t_d}^{T_c} [F_\Theta(\tau) - F_\Theta(t_d)]\mathrm{d}\tau}{T_c \cdot [\overline{F}_\Theta - F_\Theta(t_d)]} \tag{2}$$

where T_C is the time when the system is completely recovered, and the t_d is the time when the system performance reaches its floor. Fig. 1 illustrates the conceptual resilience curve by the critical functionality over the time interval of the disruptive context. The curve ALNQ in Fig. 1 reflects the system performance before, during, and after the disruptive event. Obviouly, system resilience $R(E)$ as defined by (2) is the ratio of the shaded area to the whole area of ABPQ in Fig. 1. Thus, higher value of $R(E)$ suggests better resilience of system, namely more resistant to the negative effects of the disruptive event and faster rehabilitating activities. Without loss of generality, it is further assumed that the disruptive event occurs at time 0.

As is similar to the treatment in Ganin's work [8], T_C is the control time and can be set a priori. In practical analysis, even if T_C is larger than the true full-recovery time, it will not principally cause significant distortion to analytical results. Notice that t_d can be equally regarded as the time when the rehabilitating activities are started, provided that the system will not exacerbate anymore once the rehabilitating activities are launched.

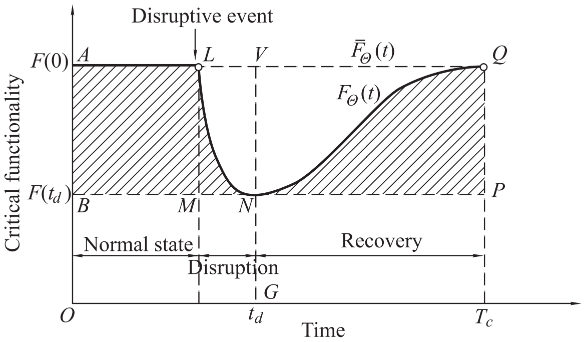

Fig. 1 Critical functionality and resilience curve

It is easy to see that larger $R(E)$ implies better resistance and faster recovery. The numerator in the last expression of (2) is the sum of two terms: the integral over $[0, t_d]$ can be regarded as static resilience, while the integral over $[t_d, T_C]$ can be regarded as dynamic resilience [27]. Clearly, the aim of post-disruption recovery strategy is to maximize $\int_{t_d}^{T_c} [F_\Theta(\tau) - F_\Theta(t_d)]\mathrm{d}\tau$. As for the discrete configuration along the time horizon, the objective function can be discretized as the sum of $F_\Theta(t) - F_\Theta(t_d)$ over time slots.

An illustrative simple network model is shown in Fig. 2, whose topology is similar to that of Réseau Express Régional-B (RER-B) railway in Paris. The numbers labeled along the links in Fig. 2(a) designate the capacity of the links, and the numbers in Fig. 2(b) designate the residual availability of links after a disruptive event, in which links l_{EF}, l_{FC}, l_{FD} are affected.

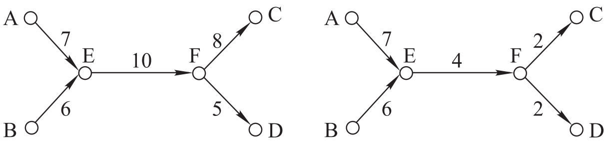

Fig. 2 Illustrative network with two fork ends

Let the benchmark O-D set $\Theta = \{\langle \mathrm{A, C}\rangle, \langle \mathrm{A, D}\rangle, \langle \mathrm{B, C}\rangle, \langle \mathrm{B, D}\rangle\}$. It can be calculated that $\overline{F}_\Theta = 7+5+6+5 = 23$, while the post-disaster critical functionality $F_\Theta(t_d) = 2+2+2+2 = 8$. In what follows, only deterministic cases are considered, i.e., the link recovery is completed in fixed time and in order of precedence. By different orders of link recovery, the critical functionality shows differences, as is summarized in Table 1.

Table 1 Critical functionality according to different recovery strategies

Strategy#	Order of recovery	Critical functionality variation
1	$l_{\mathrm{EF}} \rightarrow l_{\mathrm{FC}} \rightarrow l_{\mathrm{FD}}$	8→17→23
2	$l_{\mathrm{EF}} \rightarrow l_{\mathrm{FD}} \rightarrow l_{\mathrm{FC}}$	8→14→23
3	$l_{\mathrm{FD}} \rightarrow l_{\mathrm{EF}} \rightarrow l_{\mathrm{FC}}$	12→14→23
4	$l_{\mathrm{FD}} \rightarrow l_{\mathrm{FC}} \rightarrow l_{\mathrm{EF}}$	12→16→23
5	$l_{\mathrm{FC}} \rightarrow l_{\mathrm{FD}} \rightarrow l_{\mathrm{EF}}$	12→16→23
6	$l_{\mathrm{FC}} \rightarrow l_{\mathrm{EF}} \rightarrow l_{\mathrm{FD}}$	12→17→23

Table 1 shows that the critical functionality variation strongly depends upon the recovery order of links. In other words, the dynamic resilience of the network relies on the scheduling of the recovery operation. Notice that the scheduling is implemented by the granularity of single link recovery. This is to say, the recovery of a link is not interrupted and re-entered by the scheduling. In fact, if the scheduling is conducted with finer granularity, i.e., preemption is supported among recovery task over multiple links, more efficient results can be obtained. Nevertheless, regarding the practical operation, the analysis in the sequel sticks to the single link recovery principle, while parallel link recovery is allowed.

When the recovery scheduling problem is combined with the constraints among multiple links, the scheduling will become more intriguing and challenging, and some heuristic scheme should be developed to avoid impractical computational complexity.

3. Network analysis based recovery strategy design

3.1 Simple case of uniform recovery time

It is perceivable that the utility of recovery scheduling is determined by two major factors, namely, the current residual availability and the topology of links. The former indicates the connectivity of the link *per se*, and the latter indicates the connective features of overall interconnection. With respect to the illustrative example in Fig. 1, the simple case is firstly reviewed in which every link has identical recovery time δ slots.

Given a post-hazard scenario, according to the previous notations and assumptions, let t_d be the time slot when the system (i.e., very link) reaches its worst state. Let $F_t \subseteq L$ be the set of impaired links at time t. For the convenience of analysis, here residual availability of an impaired link is treated as a continuous real number, although it is previously discretized to maximum H link states multiplied by link capacity. Let Bd_{ij} be the instant residual availability of the link l_{ij}, then the following proposition is introduced to show the contribution of a link to the overall critical functionality.

Proposition 1 For any impaired link l_{ij} in F_t, when the link is gaining availability in the recovery process, then the partial derivative $\dfrac{\partial F_\Theta}{\partial Bd_{ij}}$ is a non-negative integer, i.e., $\dfrac{\partial F_\Theta}{\partial Bd_{ij}} \in \mathbf{Z}^+ \cup \{0\}$ or it does not exist. Hence $\dfrac{\partial F_\Theta}{\partial Bd_{ij}}$ is called the marginal utility of l_{ij}.

$\dfrac{\partial F_\Theta}{\partial Bd_{ij}}$ indicates the importance of link with respect to the instant residual availability at a given time. In fact, $\dfrac{\partial F_\Theta}{\partial Bd_{ij}}$ is the number of path where link l_{ij} is the bottleneck of the paths if the partial derivative exists.

To maximize the utility of recovery at any time slot t, each link needs to be associated with an instant precedence in the recovery process. The analysis in the sequel will show that, if the time factor is not considered, at each time slot the recovery precedence can be computed by a heuristic scheme with affordable complexity. To this end, some definitions and propositions are brought along, as follows.

Definition 1 At time slot t, let the link $l_{ij} \in F_t$ have the residual availability $RA_t(l_{ij})$, and the current system critical functionality be $F_\Theta(t)$. If at time slot $t+\delta$, link l_{ij} is recovered to its full capacity w_{ij} while the other impaired links remain their states of time slot t, so that the critical functionality is increased by $F_\Theta(t+\delta) - F_\Theta(t)$. This increment is called the recovery gain of link l_{ij} at time t, and is denoted by $G_t(l_{ij})$.

If we assume that the links are recovered in a serial manner, and the interim states of a link before full recovery are neglected, the following proposition holds by simply observing that the only two possibilities of scheduling will come to the same final critical functionality.

Proposition 2 At time slot t, for the two impaired links $l_{i_1j_1}, l_{i_2j_2}$, such that $G_t(l_{i_1j_1}) > G_t(l_{i_2j_2})$, then the optimal order of recovery is $l_{i_1j_1}, l_{i_2j_2}$.

Unfortunately, it is hard to generalize this proposition to the case of more than two links by stringent proof. Therefore, based on this proposition, a heuristic scheme is delineated in Fig. 3 to obtain the optimal scheduling without consideration of time factors. The calculation complexity at each step (time slot) is $O(|N|^2 \cdot |\Theta| \cdot |F_t|)$.

3.2 Inhomogeneous recovery time among links

3.2.1 Utility based principles

The previous analysis without considering the recovery time factor provides an intuitive understanding of the "goodness" of covering an impaired link. In practice, however, significant challenges will be elicited by the time factor of link recovery.

By observing the definition of $F_\Theta(t)$, it can be seen that the increment of $F_\Theta(t)$ is determined by the increment of the contributing links that are gaining connectivity (i.e., recovering). For a specific link l_{ij} in F_t and a given time period, the contribution of its increment to the overall critical functionality is the absolute increment multiplied by the number of paths where the increment accounts, and the number of paths is the marginal utility $\dfrac{\partial F_\Theta}{\partial Bd_{ij}}$. In fact, $\dfrac{\partial F_\Theta}{\partial Bd_{ij}}$ depends on the states of other links and thus will vary over time.

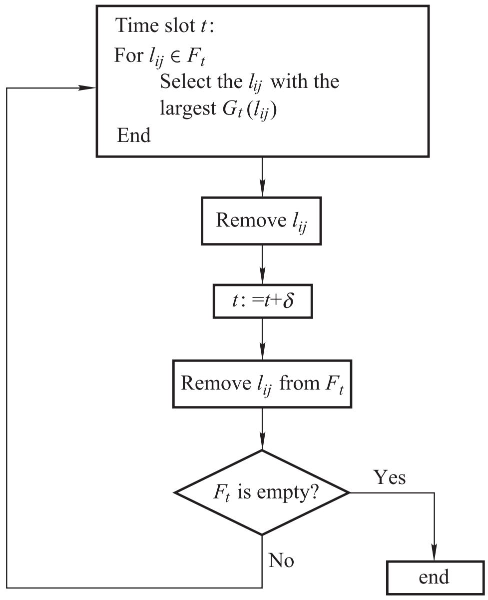

Fig. 3 A heuristic scheme of recovery scheduling under uniform recovery time assumption

The extreme case of interest is the futile recovery, i.e., $\dfrac{\partial F_\Theta}{\partial Bd_{ij}} = 0$, in which the recovery of a link does not provide any goodness to the overall critical functionality in some time periods due to the curb of other links, and this case is also called conditional confliction. Bearing this in mind, the naïve principles of scheduling should be satisfied as much as possible, i.e., the links with larger marginal utility deserves higher priority.

3.2.2 Representing the constraint by Zadeh operators

As has been defined previously, for a given $(N_p, N_q) \in \Theta$, $Wd_t(N_p, N_q)$ is obtained by the min-max calculation over series of links. Using Zadeh's operator $\wedge(\min)$, at each time slot, $Wd_t(N_p, N_q)$ can be represented by

$$Wd_t(N_p, N_q) = \sum_k [(RA_t(l_{i_1^{(k)} j_1^{(k)}}) \wedge RA_t(l_{i_2^{(k)} j_2^{(k)}}) \wedge \cdots \wedge RA_t(l_{i_{r(k)}^{(k)} j_{r(k)}^{(k)}}) \wedge C_k)] \quad (3)$$

where $l_{i_s^{(k)} j_s^{(k)}} \in F_t$, $s = 1, 2, \ldots, r(k)$, and C_k represents the connectivity of normal (non-disrupted) links corresponding to the conjunctive term, k is the number of different paths connecting N_p and N_q.

As for the example of network in Fig. 4, let $F_t = \{l_{\mathrm{CE}}, l_{\mathrm{EF}}, l_{\mathrm{FG}}, l_{\mathrm{GP}}\}$ be the set of impaired links at time slot t, and $\Theta = \{(N_S, N_T), (N_A, N_I)\}$, (3) can be instantiated as

$$Wd_t(N_S,N_T) = (RA_t(l_{\mathrm{SB}}) \wedge RA_t(l_{\mathrm{BC}}) \wedge RA_t(l_{\mathrm{CE}}) \wedge RA_t(l_{\mathrm{EF}}) \wedge RA_t(l_{\mathrm{FT}})) + (RA_t(l_{\mathrm{SB}}) \wedge RA_t(l_{\mathrm{BC}}) \wedge RA_t(l_{\mathrm{CD}}) \wedge RA_t(l_{\mathrm{DF}}) \wedge RA_t(l_{\mathrm{FT}})) + (RA_t(l_{\mathrm{SB}}) \wedge RA_t(l_{\mathrm{BC}}) \wedge RA_t(l_{\mathrm{CE}}) \wedge RA_t(l_{\mathrm{EF}}) \wedge RA_t(l_{\mathrm{FG}}) \wedge RA_t(l_{\mathrm{GQ}}) \wedge RA_t(l_{\mathrm{QH}}) \wedge RA_t(l_{\mathrm{HT}})) + (RA_t(l_{\mathrm{SB}}) \wedge RA_t(l_{\mathrm{BC}}) \wedge RA_t(l_{\mathrm{CE}}) \wedge RA_t(l_{\mathrm{EF}}) \wedge RA_t(l_{\mathrm{FG}}) \wedge RA_t(l_{\mathrm{GP}}) \wedge RA_t(l_{\mathrm{PH}}) \wedge RA_t(l_{\mathrm{HT}})) + (RA_t(l_{\mathrm{SB}}) \wedge RA_t(l_{\mathrm{BC}}) \wedge RA_t(l_{\mathrm{CD}}) \wedge RA_t(l_{\mathrm{DF}}) \wedge RA_t(l_{\mathrm{FG}}) \wedge RA_t(l_{\mathrm{GQ}}) \wedge RA_t(l_{\mathrm{QH}}) \wedge RA_t(l_{\mathrm{HT}})) + (RA_t(l_{\mathrm{SB}}) \wedge RA_t(l_{\mathrm{BC}}) \wedge RA_t(l_{\mathrm{CD}}) \wedge RA_t(l_{\mathrm{DF}}) \wedge RA_t(l_{\mathrm{FG}}) \wedge RA_t(l_{\mathrm{GP}}) \wedge RA_t(l_{\mathrm{PH}}) \wedge RA_t(l_{\mathrm{HT}})) + (RA_t(l_{\mathrm{SG}}) \wedge RA_t(l_{\mathrm{GP}}) \wedge RA_t(l_{\mathrm{PH}}) \wedge RA_t(l_{\mathrm{HT}})) + (RA_t(l_{\mathrm{SG}}) \wedge RA_t(l_{\mathrm{GQ}}) \wedge RA_t(l_{\mathrm{QH}}) \wedge RA_t(l_{\mathrm{HT}})). \quad (4)$$

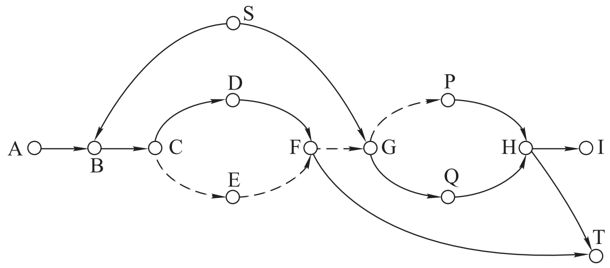

Fig. 4 An example to show the conjunctive normal formation representation

It can be rewritten as follows:

$$Wd_t(N_S,N_T) = (RA_t(l_{\mathrm{CE}}) \wedge RA_t(l_{\mathrm{EF}}) \wedge C_1) + C_2 + (RA_t(l_{\mathrm{CE}}) \wedge RA_t(l_{\mathrm{EF}}) \wedge RA_t(l_{\mathrm{FG}}) \wedge C_3) + (RA_t(l_{\mathrm{CE}}) \wedge RA_t(l_{\mathrm{EF}}) \wedge RA_t(l_{\mathrm{FG}}) \wedge RA_t(l_{\mathrm{GP}}) \wedge C_4) + (RA_t(l_{\mathrm{FG}}) \wedge C_5) + (RA_t(l_{\mathrm{FG}}) \wedge RA_t(l_{\mathrm{GP}}) \wedge C_6) + (RA_t(l_{\mathrm{GP}}) \wedge C_7) + C_8. \quad (5)$$

Similarly,

$$Wd_t(N_A,N_I) = (RA_t(l_{\mathrm{FG}}) \wedge RA_t(l_{\mathrm{GP}}) \wedge C_1') + (RA_t(l_{\mathrm{FG}}) \wedge C_2') \vee (RA_t(l_{\mathrm{CE}}) \wedge RA_t(l_{\mathrm{EF}}) \wedge RA_t(l_{\mathrm{FG}}) \wedge RA_t(l_{\mathrm{GP}}) \wedge C_3') + (RA_t(l_{\mathrm{CE}}) \wedge RA_t(l_{\mathrm{EF}}) \wedge RA_t(l_{\mathrm{FG}}) \wedge C_4') \quad (6)$$

3.2.3 Sorting the links by utility based on conjunctive clauses

The derivation in (5) and (6) provides typical instances to learn how the constraints among the impaired links and normal links go into effect. Considering there are multiple O-D pairs of interest in Θ, the recovery of this link may contribute in more than one O-D pair. The decomposition into conjunctive clauses shows that, if other impaired links remain their current states (i.e., unrepaired), the contribution of the specified link recovery to the overall critical functionality can be delineated by a piecewise function whose curve comprises a series of connected straight line segment with the slope being an integer.

It can be seen from (3), that if the recovery of a link has reached a certain value, the additional increment will be futile with respect to the specific O-D pair. This implies that, as the recovery goes on, the marginal utility of a link will decline. Fig. 5 demonstrates the outline of the curve. Some inflection points emerge as the hinges that connect the segments, and the slop of the segment decreases as the residual availability grows.

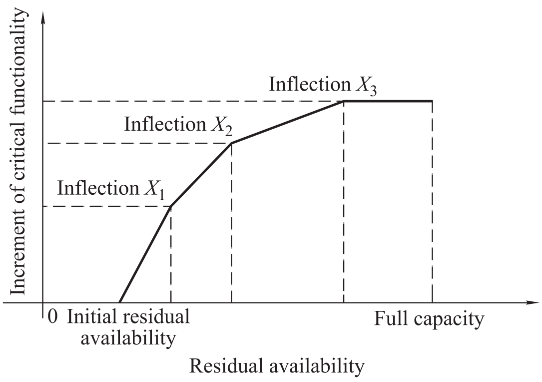

Fig. 5 Piecewise curve of the increment critical functionality against one link recovery

For a given link $l_{ij} \in F_t$, let $TTR_t(l_{ij})$ be the time to recovery (in time slots) for the link, and $G_t(l_{ij})$ is redefined as $F_\Theta(t + TTR_t(l_{ij})) - F_\Theta(t)$, i.e., the increment of critical functionality by the sole repairment of l_{ij}. We assume that the recovery process is linear, i.e., the recovery speed of a link is constant. In this regard, when time factors are taken into consideration, the raw recovery utility of l_{ij} at time slot t is defined as $\dfrac{G_t(l_{ij})}{TTR_t(l_{ij})}$, also denoted by $RU_t(l_{ij})$ for simplicity. Parallel to the scheme illustrated in Fig. 3, the recovery utility is used as a major quantitative factor to select the link that deserves the current preparation. In the real circumstance, $TTR_t(l_{ij})$

is of two-folded meaning. First, it is estimated by epistemic knowledge, and it can also stand for the actual time spent on the link to its full functionality. In the scheduling scheme, $RU_t(l_{ij}) = \dfrac{G_t(l_{ij})}{TTR_t(l_{ij})}$ is calculated for link selection, where $TTR_t(l_{ij})$ is the estimated value.

3.2.4 Pairwise modification of recovery utility among links

The recovery utility stands for the direct contribution of a link if the recovery chance is granted to it. However, the constraints among the links may give rise to the crossed complexity that is caused by the positions of the links within the multiple O-D pairs.

Considering the simple example in Fig. 6, the recovery of $l_{i_2j_2}$ is limited by the current residual availability of $l_{i_1j_1}$ regarding the pair (N_{p_2}, N_{q_2}), otherwise, the recovery of $l_{i_2j_2}$ will provide more connectivity for the overall critical functionality. Similarly, the recovery of $l_{i_1j_1}$ is limited by the current residual availability of $l_{i_3j_3}$ regarding the pair (N_{p_1}, N_{q_1}). Therefore, the recovery precedence of $l_{i_1j_1}$ over $l_{i_2j_2}$ results from a global preference with respect to the current restrictions, i.e., simultaneous consideration of (N_{p_1}, N_{q_1}) and (N_{p_2}, N_{q_2}). This suggests the hint that the raw recovery utility of l_{ij} should be further modified by a factor to reflect the "second order" contribution.

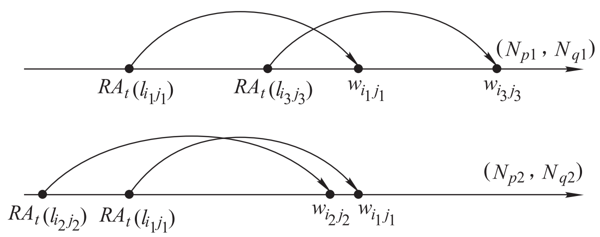

Fig. 6 A simple case of precedence due to compromise

Let $l_{i_1j_1}, l_{i_2j_2} \in F_t$ be two impaired links, $G_t(l_{i_1j_1})$ be the recovery gain of $l_{i_1j_1}$, and $G_t(l_{i_2j_2})$ be the recovery gain of $l_{i_2j_2}$. Let $G_t(l_{i_1j_1}, l_{i_2j_2})$ be the increment of critical functionality when link $l_{i_1j_1}, l_{i_2j_2}$ are recovered to their full capacity $w_{i_1j_1}, w_{i_2j_2}$ while the other impaired links remain their states of time slot t. Thus a quantitative term is needed to describe the relative mutual restriction between the two links, and this is derived by the empirical and pre-defined coefficient constants by repeated simulation experiment.

Definition 2 The relative recovery gain of $l_{i_2j_2}$ over $l_{i_1j_1}$ is $\dfrac{G_t(l_{i_1j_1}, l_{i_2j_2}) - G_t(l_{i_1j_1})}{G_t(l_{i_1j_1})}$, and is equally denoted by $RG_t(l_{i_2j_2}|l_{i_1j_1})$ provided $G_t(l_{i_1j_1}) \neq 0$; inversely, the relative superiority of $l_{i_1j_1}$ over $l_{i_2j_2}$ is $\dfrac{G_t(l_{i_1j_1})}{G_t(l_{i_1j_1}, l_{i_2j_2}) - G_t(l_{i_1j_1})}$, and is equally denoted by $RS_t(l_{i_2j_2}|l_{i_1j_1})$ provided $G_t(l_{i_1j_1}, l_{i_2j_2}) \neq G_t(l_{i_1j_1})$.

Intuitively, $RS_t(l_{i_2j_2}|l_{i_1j_1})$ describes the "goodness" that $l_{i_1j_1}$ should be recovered ahead of $l_{i_2j_2}$. However, four extreme cases should be noticed as follows:

Case 1: $G_t(l_{i_1j_1}, l_{i_2j_2}) = G_t(l_{i_1j_1}) \neq 0$

In this case, the recovery of $l_{i_2j_2}$ after $l_{i_1j_1}$ is zero. It can be easily seen that if $l_{i_2j_2}$ is recovered ahead of $l_{i_1j_1}$, $G_t(l_{i_2j_2})$ is 0. Therefore $RS_t(l_{i_2j_2}|l_{i_1j_1})$ is set to be $+\infty$.

Case 2: $G_t(l_{i_1j_1}) = 0$, $G_t(l_{i_1j_1}, l_{i_2j_2}) \neq 0$

In this case, the recovery of $l_{i_1j_1}$ before $l_{i_2j_2}$ is futile, therefore $RS_t(l_{i_2j_2}|l_{i_1j_1}) = 0$.

Case 3: $G_t(l_{i_1j_1}, l_{i_2j_2}) = G_t(l_{i_1j_1}) = G_t(l_{i_2j_2}) = 0$

In this case, neither $l_{i_1j_1}$ nor $l_{i_2j_2}$ can contribute to the overall critical functionality. Set $RS_t(l_{i_2j_2}|l_{i_1j_1}) = 0$ for conformation.

Case 4: $RG_t(l_{i_1j_1}|l_{i_1j_1})$ is set to be 1

Considering that the value range of $RS_t(l_{i_2j_2}|l_{i_1j_1})$ is $[0, +\infty]$, to obtain a computable and controllable term, the normalized relative superiority is introduced as below.

Definition 3 The normalized relative superiority of $l_{i_1j_1}$ over $l_{i_2j_2}$, denoted by $\overline{RS}_t(l_{i_2j_2}|l_{i_1j_1})$, which maps the relative superiority to the interval [0,1] by hyperbolic tangent:

$$\overline{RS}_t(l_{i_2j_2}|l_{i_1j_1}) = \tanh[RS_t(l_{i_2j_2}|l_{i_1j_1})]$$

where $\overline{RS}_t(l_{i_2j_2}|l_{i_1j_1}) = 1$ if $G_t(l_{i_1j_1}, l_{i_2j_2}) = G_t(l_{i_1j_1}) \neq 0$, corresponding to Case 1.

Literally, $\overline{RS}_t(l_{i_2j_2}|l_{i_1j_1})$ illustrates the confidence that $l_{i_1j_1}$ should be recovered ahead of $l_{i_2j_2}$. If $F_t = \{l_{i_sj_s}\}$, $s = 1, 2, \ldots, S$, which has S impaired links, the modification matrix is used to refine the raw recovery utility of the links. Correspondingly, $RU_t(l_{i_1j_1}) \cdot \sum\limits_{\tau=1}^{S} \overline{RS}_t(l_{i_\tau j_\tau}|l_{i_1j_1})$ indicates the integrated confidence that $l_{i_1j_1}$ should be given the recovery priority among all the links. Referring to the heuristic scheme delineated in Fig. 2, the current link recovery at time slot t should be link $l_{i_{\hat{v}}j_{\hat{v}}}$ such that

$$\hat{v} : \max_{v} \left\{ RU_t(l_{i_vj_v}) \cdot \sum_{\tau=1}^{S} \overline{RS}_t(l_{i_\tau j_\tau}|l_{i_vj_v}) \right\}.$$

3.2.5 Uncertainty in recovery time of links

In practical operation, the recovery time for a link is usually associated with uncertainty. In this regard, $TTR_t(l_{ij})$ is a stochastic variable. As the recovery time for a link is subject to diverse factors, it is normally predicted with empirical or epistemic knowledge. If the $TTR_t(l_{ij})$ can be known to conform to a certain distribution, i.e., $P(TTR_t(l_{ij}) = k) = p_k$ $(k = 1, 2, \ldots)$. Obviously,

p_k is dependent upon l_{ij}, and the current degree of status $RA_t(l_{ij})$. With this stochastic setup, the optimization problem can be interpreted in the sense of expectation, as follows:

$$\max \mathrm{E}\left[\sum_{t=t_d}^{T_c}(F_\Theta(t) - F_\Theta(t_d))\right].$$

To obtain a revised dynamic scheme for the optimal problem, we simply redefine the $RU_t(l_{ij}) = \dfrac{G_t(l_{ij})}{\mathrm{E}[TTR_t(l_{ij})]}$ and keep most of the previous scheduling principles unchanged.

4. An illustrative example based on Monte Carlo simulation

4.1 Background of the illustrative example

Fig. 7 demonstrates the backbone network of Wuhan, a metropolis in the geographic center of China. The city is divided by Yangtze River and its branch Han River. Currently, there are seven bridges on the Yangtze River to share the high demand of cross-river traffic. Meanwhile, there are several regional transit points on both sides of the Yangtze River inside the city, and traffic among these transit points constitute a major demand that shapes the traffic patterns. The backbone roads are subject to some aleatory disruptions such as vehicle accidents, temporary construction or maintenance of road assets, which cause degradation to the overall connectivity.

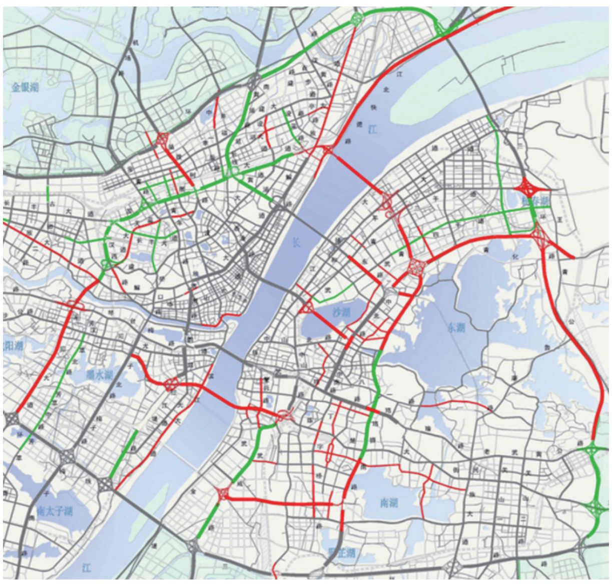

Fig. 7 Backbone road network of Wuhan

Fig. 8 focuses on one of the typical traffic patterns to investigate the recovery strategy in terms of throughput across the network. Thirty nodes and 46 links are extracted to characterize the backbone road network. The numbers in the brackets indicate the width of the links, and the non-bracketed numbers are the labels of the nodes. The one-way pattern reflects the traffic from the west (north side of Yangtze River) to the east (south side of Yangtze River). Let the O-D pairs of interests be $\Theta = \{(N_5, N_{24}), (N_5, N_{25}), (N_5, N_{30}), (N_7, N_{25}), (N_7, N_{30}), (N_4, N_{27}), (N_4, N_{28}), (N_8, N_{30})\}$, the set shows the special concern with the connectivity among some of the local transit points across the Yangtze River. The road network features the multi-state for each link of the graph, and this implies that the increment of a link's residual availability will contribute to the critical functionality of the whole network.

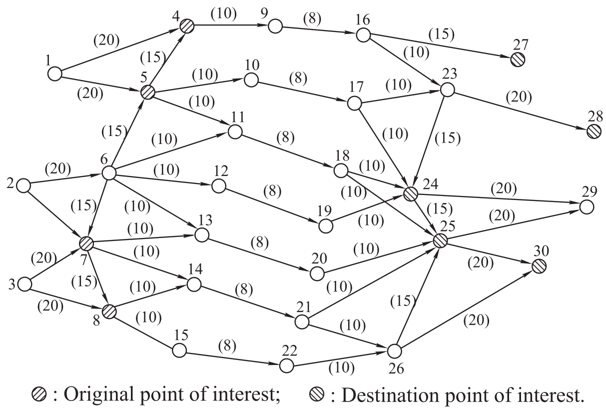

Fig. 8 Graph representation of the network focusing on one-direction traffic

4.2 Basic practicability of the scheme

To demonstrate the validity of the proposed scheme, the basic configuration of the simulation is set as follows: the links are subjective to a common random failure rate (i.e., undergoing a disruption); when a link is randomly selected as disrupted, its instant residual availability confirms to half-normal distribution (i.e., the absolute value of a normal distribution) with truncation to the interval (0,1), indicating the percentage of availability; the recovery time is also generated by half-normal distribution with a coefficient of $(1 - RA_t(l_{ij}))$ to show that lower residual availability leads to longer recovery time in average; the epistemic uncertainty of recovery time is the "true recovery time" deviated by a stochastic term ε conforming to a truncated normal distribution.

Fig. 9 shows the result of 20 repeated simulations when a randomly generated impaired ensemble is fixed. The Monte Carlo simulation includes the epistemic knowledge about the recovery time and the random sequence in the non-optimized scheme. The advantage of the proposed scheme over the pure random scheme is obvious in terms of recovery efficiency, as is compared in Fig. 10.

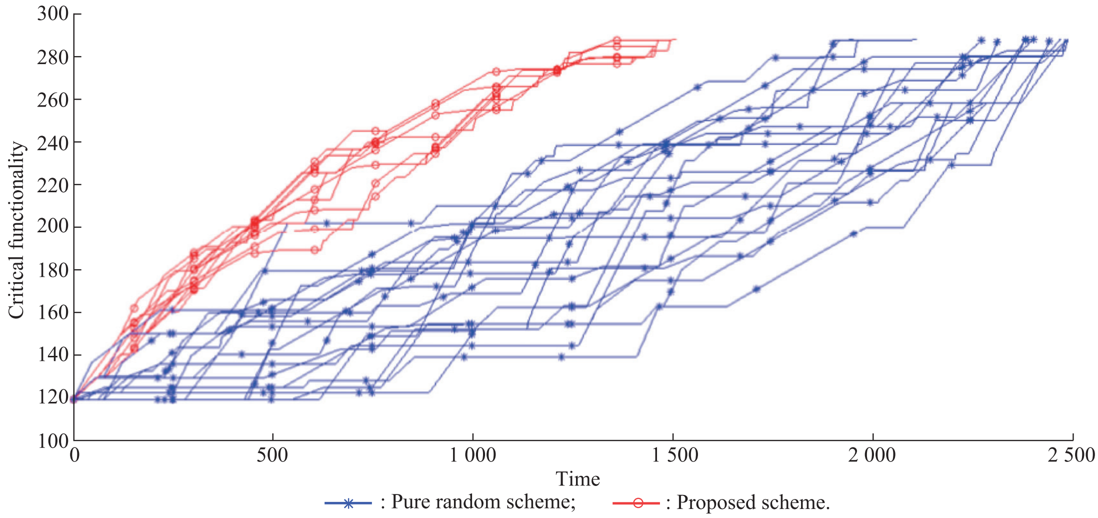

Fig. 9 Critical functionality of Monte Carlo simulation

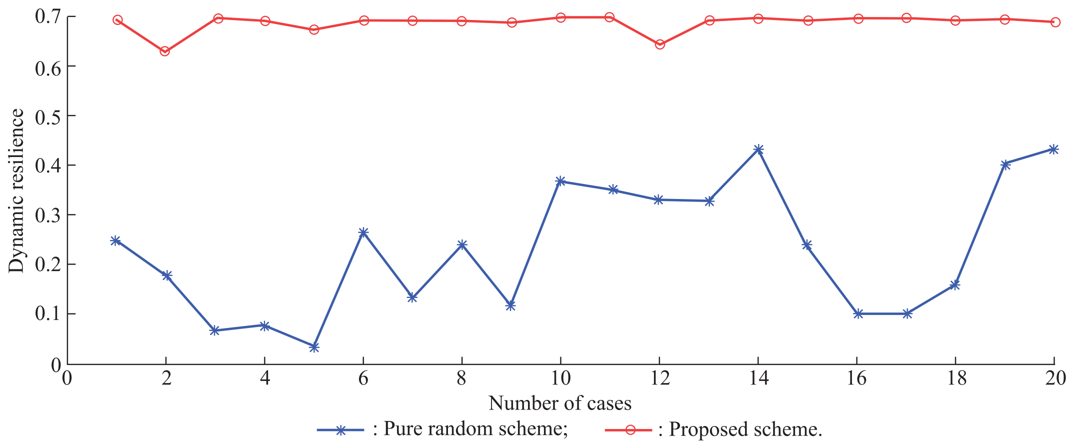

Fig. 10 Comparison of dynamic resilience

4.3 Dependence on the epistemic uncertainty

The simulation test described in the previous section provides a glance at the feasibility of the proposed algorithm. In real circumstances, the states of the impaired links are partially known, i.e., we can know about which links are affected by the adverse event, while the recovery time of the links can only be estimated. This gives rise to the epistemic uncertainty when the proposed scheme is implemented.

When combined with the aforementioned epistemic uncertainty, two concerns of the scheme should be of special interests: first, if the recovery time can be accurately obtained, what will the performance of the scheme be like? Second, what is the sensitiveness of the performance of the scheme with regard to different epistemic knowledge? As the proposed schemed is largely heuristic, Monte Carlo simulation is once more used to test the two aspects of the problem.

Fig. 11 provides an exhaustive experiment against the proposed scheme. Eight links are randomly selected as being impaired, with the residual availability and the recovery time generated by rules described in Section 4.2. With all these configurations fixed, the permutation of recovery orders are all tried, in addition to the recovery order calculated by the proposed scheme. This is to say, 40 320 recoveries options are exploited. The red line shows the critical functionality calculated by the proposed scheme, other blue lines represent the critical functionality of the rest recovery options. Although the proposed scheme is heuristic in principle, its performance is very promising in this test case.

It is worth mentioning that, in this test, the residual availability and the recovery time is presumed to be complete and accurately known, which constitute the input to the proposed scheme. However, in real circumstances, this assumption will yield its way to epistemic uncertainties and estimation errors. Hence further experiment is conducted to test the stability of the scheme against the uncertainties.

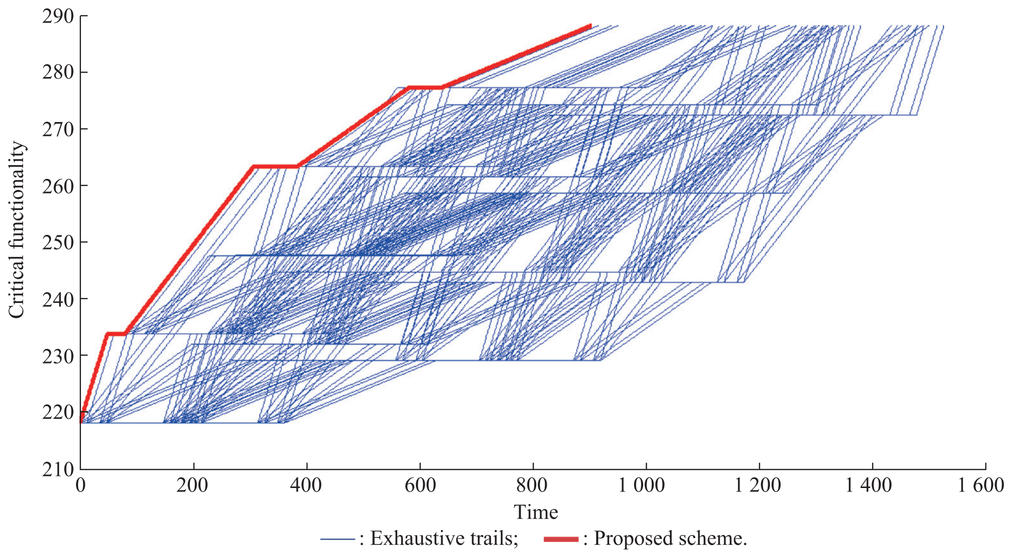

Fig. 11 Performance of the proposed scheme compared to exhaustive trails

4.4 Dependence on the epistemic uncertainty

Several suits of tests are performed to investigate to what extent the deviation of the recovery time estimation for the impaired links can affect the results calculated from the "perfect knowledge". In these tests, 16 links are randomly selected as the impaired links, with similar simulation configuration as described in Section 4.2. To determine the $TTR_t(l_{ij})$ at each step, some distortion is added to the true recovery time of the link to simulate the epistemic uncertainties about the actual value, which is presented by two parameters, namely the mean (M) and the variance (Var). M refers to the ratio of the estimated time against the actual time, and Var indicates the deviation of the simulated $TTR_t(l_{ij})$ from its mean. For each suit of test, 20 independent repetitions are conducted. Table 2 summarizes the 10 variations of the inputs and the corresponding output results. The results suggest that the proposed scheme is very stable regarding the error between the epistemic estimated and the actual TTR. The variance of epistemic errors indicated in the far-left column causes very slight degradation of the results in terms of mean dynamic resilience and variance. Fig. 12 displays the sample critical functionality curves generated by the configurations. The curve in thick red refers to scheduling by perfect knowledge, and many curves overlap into one, which further implies the stability of the proposed scheme. It should be noticed that some extreme cases still exist, which shows considerable degradation in dynamic resilience.

Table 2 Simulation of the epistemic *TTRs* for 16 impaired links to test the stability of the proposed scheduling scheme

Input	Output		
Mean and variation of the epistemic knowledge about recovery time	Mean of dynamic resilience	Mean of dynamic resilience compared with perfect knowledge	Variation of resilience
M=1.4, Var=0.12	0.819	0.999	0.002
M=1.2, Var=0.12	0.817	0.997	0.004
M=1.0, Var=0.12	0.815	0.994	0.005
M=0.8, Var=0.12	0.806	0.984	0.010
M=0.6, Var=0.12	0.781	0.953	0.035
M=1.4, Var=0.03	0.819	1.000	0.000
M=1.2, Var=0.03	0.819	1.000	0.000
M=1.0, Var=0.03	0.819	1.000	0.000
M=0.8, Var=0.03	0.818	0.998	0.003
M=0.6, Var=0.03	0.818	0.998	0.003

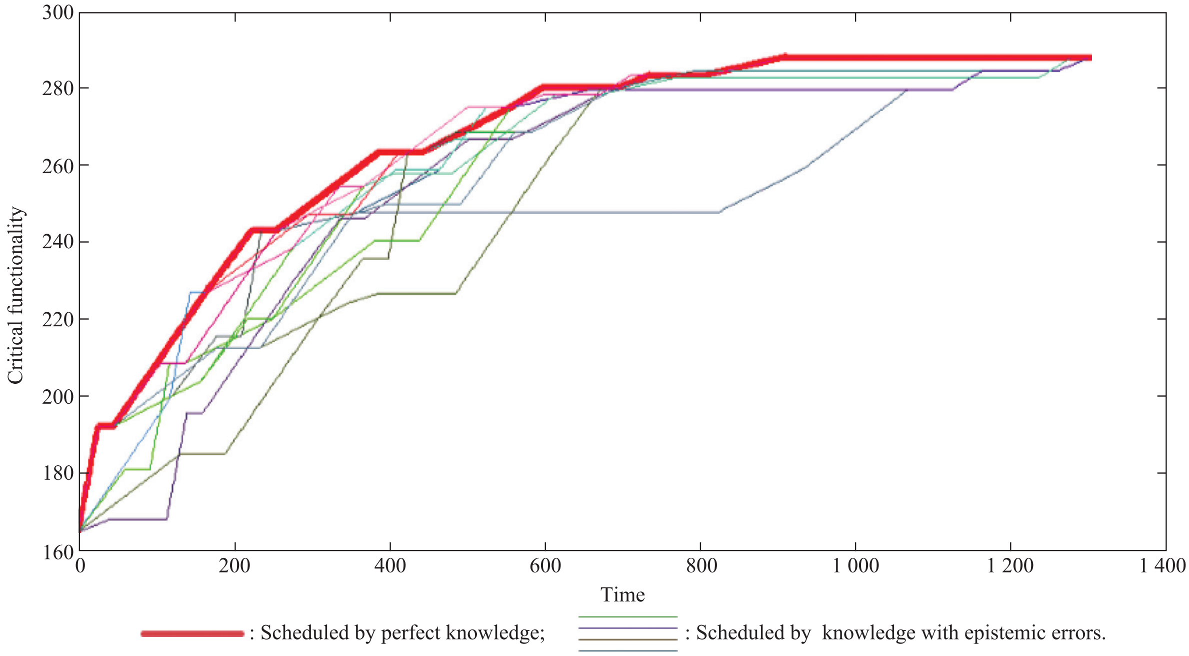

Fig. 12 Simulation of sensitivity test caused by epistemic error about *TTR*

4.5 Some remarks on the proposed scheme in contrast with the previous CI study

As introduced in the literation review, CI has influenced previous research [28]. In fact, CIM has been a classical research topic in system reliability studies [29,30], and some stereotyped measures are formed, such as Birnbaum's measure, and Fussell-Vesely's measure [31,32]. These studies mainly focus on the ex-ante analysis, with strong dependence on structural nature of the system and the prior knowledge (such as prior probability) about the survivability of individual components.

Recently, driven by the system resilience research for critical infrastructures, a shift of paradigm emerges in CIM study [19 – 21], which is referred to as resilience-based CIM in the sequel. The resilience-based CIM study generally consists of two phases: firstly, the goal is to search for the strategy of the recovery process that can reach the maximization of system resilience; secondly, based on the recovery priority of the individual components, the resilience-based CIM can then be calculated according to the rankings of the component priority by predefined criteria. The presented work in this paper can be categorized into the optimization phase, in which the order of component recovery is rendered by the scheme. It is worth mentioning that the recovery order of the links is subject to several factors, including the topology feature of the impaired links, the magnitude of the damage to the links and the time cost of each individual link. Thus, the resilience-based CIM of the links strongly depends on the post-disruption scenario of the adverse event. This will result in more dynamic CIM values compared to the classical ex-ante CIM.

4.6 Advantages of dynamic scheduling

The basic idea of the proposed scheme is to adopt dynamic selection of the most critical link instead of determining a static scheme of restoration, i.e., a fixed order of link recovery. This paradigm has shown its advantage in the exhaustive tests as have been discussed in the previous section.

In the real circumstances where uncertainties have to be taken into consideration, the strengths of the dynamic scheduling can also be obvious.

In the fixed recovery method, the priority of link recovery is sorted by the CIM. In prior research, the Copeland Score method is widely employed to calculate CIM for link importance [20,21]. To test the validity of the proposed scheme, the Copeland Score method is also used as a candidate scheme.

Let $l_{i_1j_1}, l_{i_2j_2} \in F_t$ be two impaired links, the kth comparison of the link is given by

$$C_k(l_{i_1j_1}, l_{i_2j_2}) = \begin{cases} C_{k-1}(l_{i_1j_1}, l_{i_2j_2}) + 1, & q_k(l_{i_1j_1}) > q_k(l_{i_2j_2}) \\ C_{k-1}(l_{i_1j_1}, l_{i_2j_2}) - 1, & q_k(l_{i_1j_1}) < q_k(l_{i_2j_2}) \\ C_{k-1}(l_{i_1j_1}, l_{i_2j_2}), & q_k(l_{i_1j_1}) = q_k(l_{i_2j_2}) \end{cases}$$
$$C_0(l_{i_1j_1}, l_{i_2j_2}) = 0$$

where $k = 1, 2, \dots, \Omega$ stands for the specific attribute of the links, and totally Ω attributes are considered.

In the context of the problem, the kth attribute of the links are the kth recovery percentile starting from the residual availability. At time slot t, the associated q_k is the gain of overall critical functionality when the link l_{ij} is recovered to its partial capacity, i.e., $Res(l_{ij}) + k \cdot RecoveryStep$, while the other links remain unchanged. $Res(l_{ij})$ stands for the instant residual availability of the link, and the $RecoveryStep$ stands for the mount of progress in the recovery process, as is depicted in Fig. 13.

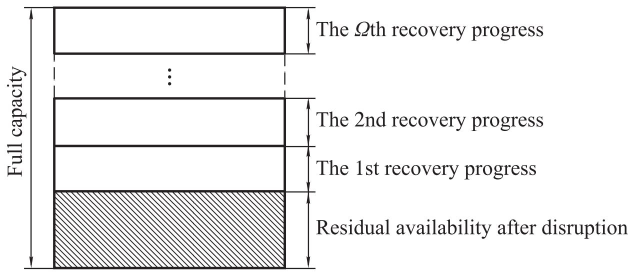

Fig. 13 Attributes of a link

The Copeland Score of a link is finally computed by

$$\mathrm{CS}(l_{ij}) = \sum_{l_{pq} \neq l_{ij}} C_{\Omega}(l_{ij}, l_{pq}).$$

The Copeland Score of a link reflects the static importance of the link. Therefore, from the static point of view, the recovery order of the links is determined by the CS value of the link.

In the Monte Carlo simulation, eight links are randomly selected as impaired, and the disruption results in the partial functionality of the links as illustrated in Table 3. The Copeland Scores of the impaired links are depicted in Fig. 14. The recovery order thus is implied by their importance value.

In the further simulation tests, the recovery time of the links are also given by half-normal distribution. Since the precedence of the links <6→7>, <6→13>, <16→27> and <22→26> are equal in terms of their Copeland Score, the simulation tests include some permutations of the four links.

Table 3 Configuration of the Monte Carlo simulation

Link	Disruption	Half-normal distribution of recovery time $\widetilde{T}$ (30,1)
5→10	0.617	$(1-0.617)\widetilde{T}$
6→7	0.033	$(1-0.033)\widetilde{T}$
6→13	0.819	$(1-0.819)\widetilde{T}$
7→13	0.107	$(1-0.107)\widetilde{T}$
8→15	0.211	$(1-0.211)\widetilde{T}$
16→27	0.707	$(1-0.707)\widetilde{T}$
21→25	0.486	$(1-0.486)\widetilde{T}$
22→26	0.866	$(1-0.866)\widetilde{T}$

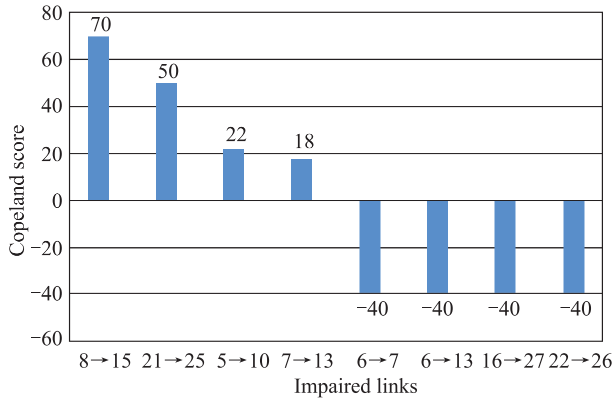

Fig. 14 Static importance order of the impaired links

Fig. 15 demonstrates the time requirement against the degree of network restoration in a typical test suit. The red curve demonstrates the proposed scheme, and the blue curves stands for the Copeland Score methods. The advantage of the proposed scheme is very evident. In this typical test suit, the recovery scheme calculated by the proposed scheme is <21→25>, <8→15>, <7→13>, <5→10>, <6→13>, <6→7>, <16→27>, <22→26>. There is considerable difference between the proposed result and the recovery strategy based on the Copeland Score as depicted in Fig. 14.

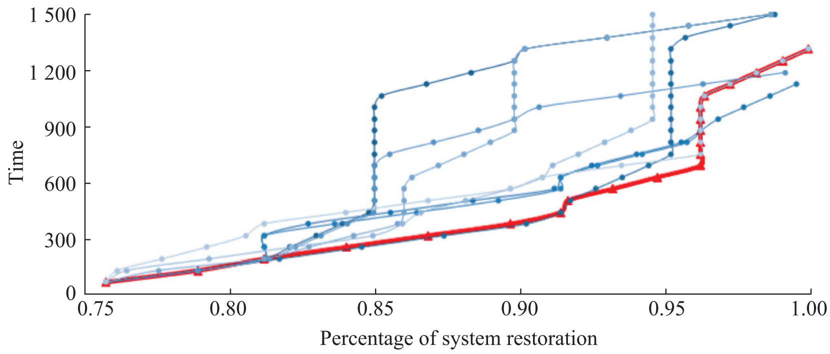

Fig. 15 Comparison of system restoration time requirement

5. Conclusions

This paper aims to devise a practical scheme to schedule the recovery process such that the dynamic resilience performance of the network system can be optimized. A heuristic scheme is proposed and tested by various configurations of Monte Carlo simulations. The simulation result shows that the proposed scheme can produce very promising result, and good accommodation with epistemic errors. For the future study, two endeavors will be carried out: firstly, the scheduling and resources allocation for parallel recovery among multiple links; secondly, constructing a larger scale of simulation tests to find the patterns of resilience-based CIMs among links which can in turn shed light on the ex-ante CIM.

References

[1] ZIO E. Challenges in the vulnerability and risk analysis of critical infrastructures. Reliability Engineering & System Safety, 2016, 152: 137 – 150.

[2] BOCCALETTI S, LATORA V, MORENO Y, et al. Complex networks: structure and dynamics. Physics Reports, 2006, 424(4): 175 – 308.

[3] FERRARIO E, PEDRONI N, ZIO E. Evaluation of the robustness of critical infrastructures by hierarchical graph representation, clustering and Monte Carlo simulation. Reliability Engineering & System Safety, 2016, 155: 78 – 96.

[4] Council of the Society for Risk Analysis. SRA develops glossary of risk-related terms. [2018-10-15]. http://www.sra.org/sites/default/files/pdf/SRA-glossary-approved22june2015-x.pdf.

[5] SUTER M. Resilience and risk management: exploring the relationship and comparing its use. Zurich: Center for Security Studies, 2011.

[6] RIGHI A W, SAURIN T A, WACHS P. A systematic literature review of resilience engineering: research areas and a research agenda proposal. Reliability Engineering & System Safety, 2015, 141: 142 – 152.

[7] CUTTER S L, AHEARN J A, AMADEI B, et al. Disaster resilience: a national imperative. Environment Science & Policy for Sustainable Development, 2013, 55(2): 25 – 29.

[8] GANIN A A, MASSARO E, GUTFRAIND A, et al. Operational resilience: concepts, design and analysis. Scientific Reports, 2016, DOI: 10.1038/srep19540.

[9] LINKOV I, BRIDGES T, CREUTZIG F, et al. Changing the resilience paradigm. Nature Climate Change, 2015, 4(6): 407 – 409.

[10] HOSSEINI S, BARKER K, RAMIREZ-MARQUEZ J E. A review of definitions and measures of system resilience. Reliability Engineering & System Safety, 2016, 145: 47 – 61.

[11] GAO J X, BARZEL B, BARABÁSI A L. Universal resilience patterns in complex networks. Nature, 2016, 530(7590): 307 – 312.

[12] ZHANG X G, MAHADEVAN S S, SANKARARAMAN S, et al. Resilience-based network design under uncertainty. Reliability Engineering & System Safety, 2018, 169: 364 – 379.

[13] REGGIANI A. Network resilience for transport security: some methodological considerations. Transport Policy, 2013, 28(7): 63 – 68.

[14] BHAVATHRATHAN B K, PATIL G R. Quantifying resilience using a unique critical cost on road networks subject to recurring capacity disruptions. Transportmetrica, 2015, 11(9): 836 – 855.

[15] WHITSON J C, RAMIREZ-MARQUEZ J E. Resiliency as a component importance measure in network reliability. Reliability Engineering & System Safety, 2009, 94(10): 1685 – 1693.

[16] NATVIG B, HUSEBY A B, REISTADBAKK M O. Measures of component importance in repairable multistate systems-a numerical study. Reliability Engineering & System Safety, 2011, 96(12): 1680 – 1690.

[17] ROSE A. Economic resilience to natural and man-made disasters: multidisciplinary origins and contextual dimensions. Environmental Hazards, 2007, 7(4): 383 – 398.

[18] ROSE A. Defining and measuring economic resilience to disasters. Disaster Prevention & Management, 2004, 13(4): 307 – 314.

[19] BARKER K, RAMIREZ-MARQUEZ J E, ROCCO C M. Resilience-based network component importance measures. Reliability Engineering & System Safety, 2013, 117(2): 89 – 97.

[20] BAROUD H, RAMIREZ-MARQUEZ J E, BARKER K, et al. Stochastic measures of network resilience: applications to waterway commodity flows. Risk Analysis, 2014, 34(7): 1317 – 1335.

[21] FANG Y P, PEDRONI N, ZIO E. Resilience-based component importance measures for critical infrastructure network systems. IEEE Trans. on Reliability, 2016, 65(2): 502 – 512.

[22] MARSEGUERRA M, ZIO E, PODOFILLINI L, et al. Optimal design of reliable network systems in presence of uncertainty. IEEE Trans. on Reliability, 2005, 54(2): 243 – 253.

[23] WU B, YAN X P, WANG Y, et al. An evidential reasoning-based CREAM to human reliability analysis in maritime accident process. Risk Analysis, 2017, 37(10): 1936 – 1957.

[24] ERIC D V, MARK A T, NATHANAEL J K. Optimal recovery sequencing for enhanced resilience and service restoratioin in transportation networks. International Journal of Critical Infrastructures, 2014, 10(3/4): 218 – 246.

[25] HENRY D, RAMIREZ-MARQUEZ J E. Generic metrics and quantitative approaches for system resilience as a function of time. Reliability Engineering & System Safety, 2012, 99: 114 – 122.

[26] LU C C, ZHOU X, ZHANG K. Dynamic origin – destination demand flow estimation under congested traffic conditions. Transportation Research Part C: Emerging Technologies, 2013, 34: 16 – 37.

[27] PANT R, BARKER K, ZOBEL C W. Static and dynamic metrics of economic resilience for interdependent infrastructure and industry sectors. Reliability Engineering & System Safety, 2014, 125(5): 92 – 102.

[28] ZIO E, PODOFILLINI L. Importance measures and genetic algorithms for designing a risk-informed optimally balanced system. Reliability Engineering & System Safety, 2007, 92(10): 1435 – 1447.

[29] ZIEGEL E R. System reliability theory: models, statistical methods, and applications. Technometrics, 2003, 46(4): 495 – 496.

[30] KUO W, ZHU X. Some recent advances on importance measures in reliability. IEEE Trans. on Reliability, 2012, 61(2): 344 – 360.

[31] BORGONOVO E. Differential, criticality and Birnbaum importance measures: an application to basic event, groups and SSCs in event trees and binary decision diagrams. Reliability Engineering & System Safety, 2007, 92(10): 1458 – 1467.

[32] MENG F C. Relationships of Fussell-Vesely and Birnbaum importance to structural importance in coherent systems. Reliability Engineering & System Safety, 2000, 67(1): 55 – 60.

Biographies

WANG Yang was born in 1976. He received his B.S. degree in mathematics from Wuhan University in 1997, M.S. degree in applied mathematics from Shanghai Jiao Tong University in 2000, and Ph.D. degree in computer science from Huazhong University of Science and Technology in 2008. He is currently an associate professor in Intelligent Transportation Systems Research Center of Wuhan University of Technology. His main research interest is transportation safety, including system resilience, risk assessment and emergency disposition. He is also conducting research on the human factors in the transportation system by developing simulation environment for human-machine interaction measurement and group performance modeling.
E-mail: wangyang.itsc@whut.edu.cn

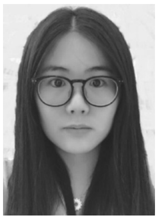

FU Shanshan was born in 1987. She received her B.E. degree in logistics engineering, M.S. degree in intelligent transportation engineering and Ph.D. degree in vehicle operation engineering from Wuhan University of Technology in 2010, 2013 and 2017 respectively. She was a research assistant at National Engineering Research Center for Water Transport Safety, from 2012 to 2016. She is currently a lecturer in the College of Ocean Science and Engineering, Shanghai Maritime University. Her main research interests include resilience analysis of transportation systems, risk modeling of arctic shipping and uncertainty modeling in quantitative risk assessment.
E-mail: fushanshan_lemon@163.com

WU Bing was born in 1986. He received his B.E. degree in navigation technology from School of Navigation, M.E. degree in traffic information engineering and control from School of Navigation, and Ph.D. degree in traffic engineering from School of Energy and Power Engineering, Wuhan University of Technology in 2008, 2012, and 2016 respectively. During the period from 2014 to 2015, he was a joint Ph.D. student in University of Lisbon. He is currently an assistant professor in Intelligent Transportation System Center of Wuhan University of Technology. His main research interests include risk analysis, decision making and human reliability analysis for transportation systems.
E-mail: bing.wu@whut.edu.cn

HUANG Jinhui was born in 1992. He received his B.E. degree in energy power system and automation from School of Energy and Power Engineering, Wuhan University of Technology in 2015. He is currently a master student in major of traffic and transportation engineering at Wuhan University of Technology. His main research interests include traffic accident modeling, organization resilience analysis, performance evaluation of emergency disposal and related fields.
E-mail: huangjinhui@whut.edu.cn

WEI Xiaoyang was born in 1990. He received his B.E. degree in navigation technology from School of Navigation, M.E. degree in communication and transportation engineering from School of Energy and Power Engineering, Wuhan University of Technology in 2014 and 2017 respectively. He is currently a Ph.D. student in Department of Civil and Environmental Engineering, National University of Singapore. His main research interests include machine learning, risk analysis and accident consequence assessment for transportation systems.
E-mail: weixiaoyang@u.nus.edu